Author(s): Achim, C. V. & Karttunen, M. & Elder, K. R. & Granato, E. & Ala-Nissilä, Tapio & Ying, S. C.

Title: Phase diagram of pinned lattices in the phase field crystal model

Year: 2008

Version: Final published version

Please cite the original version:

Achim, C. V. & Karttunen, M. & Elder, K. R. & Granato, E. & Ala-Nissilä, Tapio & Ying, S. C. 2008. Phase diagram of pinned lattices in the phase field crystal model. Journal of Physics: Conference Series. Volume 100, Issue 7. 072001. 1742-6588 (printed). DOI: 10.1088/1742-6596/100/7/072001.

Phase diagram of pinned lattices in the phase field crystal model

2008 J. Phys.: Conf. Ser. 100 072001

(http://iopscience.iop.org/1742-6596/100/7/072001)

Journal of Physics: Conference Series **100** (2008) 072001 doi:10.1088/1742-6596/100/7/072001

Phase diagram of pinned lattices in the phase field crystal model

C. V. Achim[1], M. Karttunen[2], K.R. Elder[3], E. Granato[4], T. Ala-Nissila[1,5] and S.C. Ying[5]

[1] Laboratory of Physics, Helsinki University of Technology, P.O. Box 1100, FIN-02015 TKK, Finland
[2] Department of Applied Mathematics, The University of Western Ontario, London (ON), Canada
[3] Department of Physics, Oakland University, Rochester, Michigan, 48309-4487, USA
[4] Laboratório Associado de Sensores e Materiais, Instituto Nacional de Pesquisas Espaciais, São José dos Campos, SP Brazil
[5] Department of Physics, Brown University, Providence, R.I. 02912-1843, USA

E-mail: cva@fyslab.hut.fi

Abstract. We study the phase diagram and the commensurate-incommensurate phase transitions of a two-dimensional phase field crystal model for adsorbed layers. The model allows for both elastic and plastic deformations on atomic and diffusive time-scales, and provides a continuum description of lattice systems, such as adsorbed atomic layers or two-dimensional vortex lattices. Analytically, mode expansion analysis and numerical minimization of the free energy are used to determine the ground states as a function of the pinning potential and lattice mismatch parameter. The results show a rich phase diagram with several different types of commensurate and incommensurate phases.

1. Introduction

Many systems in nature possess two or more competing length scales. Such systems often exhibit commensurate-incommensurate transitions, which are characterized by structural changes induced by the competition between these scales [1]. Examples of such systems include spin and charge density waves [2, 3], vortex lattices in superconducting films [4] and weakly adsorbed monolayers on a substrate [5]. All these systems are characterized by an order parameter ψ (e.g. charge or density wave, density of superconducting electrons, or mass density) which is modulated with a periodicity a which is usually incommensurate with the underlying lattice (of periodicity b). The interaction with the substrate is characterize by the coupling strength V_0. In a 1D system, we have a commensurate phase if the ratio between the average period $\tilde{a}$ of the order parameter and b is a rational number, while in the opposite case the phase is incommensurate with the underlying lattice.

In this study we extend the work started in Ref. [6], where we considered a 2D system described by the phase field crystal (PFC) model [7, 8]. The effect of the underlying lattice is realized by a periodic potential which is linearly coupled to the order parameter. Such a model should provide a suitable continuum description of many lattice systems such as weakly adsorbed overlayers or 2D vortex lattices. The commensurate incommensurate-transitions are induced by varying the pinning strength V_0 and the periodicity of the potential b.

2. Model

The system is described by the PFC free-energy for an adsorbed monolayer [6],

$$F = F_0 \int d^2\vec{x} \left[\frac{\psi(\vec{x})}{2}((r + (1 + \nabla^2)^2)\psi(\vec{x}) + \frac{\psi(\vec{x})^4}{4} + \psi(\vec{x})\, V(\vec{x}) \right]. \quad (1)$$

where $\psi(\vec{x})$ is a continuous field representing the number density of the adsorbed layer, and $V(\vec{x})$ represents an effective potential due to the substrate. The constant F_0 sets the scale for the energies, while r is an effective temperature which together with the average density $\bar{\psi} = (1/S)\int d^2\vec{x}\psi(\vec{x})$ determines the phase diagram in the absence of a pinning potential [7, 8].

We consider a pinning potential $V(\vec{x})$ with square symmetry

$$V(\vec{x}) = V_0 \left[\cos(k_s x) + \cos(k_s y)\right], \quad (2)$$

where $k_s = 2\pi/b$ is the wave vector of the pinning potential. The parameters r and $\bar{\psi}$ are chosen so that in the absence of the pinning potential the system is a hexagonal state with a lattice constant a_t and a wave vector $k_t = 2\pi/(a_t\sqrt(3)/2)$, *i.e.*, $r = -1/4$ and $\bar{\psi} = -1/4$, which is incommensurate with the pinning potential. The lattice mismatch between the adsorbate and substrate is defined as $\delta_{\rm m} = (k_t - k_s)/k_t$ (for the free-energy given by Eq. (1) $k_t = 1$). In Ref. [6] only $\delta_{\rm m} > 0$ was considered, and only the boundary between incommensurate and commensurate phase was shown. In this research we extend our previous work to $\delta_{\rm m} < 0$. Also in the phase diagram all the commensurate phases and the boundaries between them are shown.

Numerically, the equilibrium configurations (minimum energy states) can be found by solving a conserved equation of motion:

$$\frac{\partial\psi(\vec{x},t)}{\partial t} = \nabla^2 \left[((r + (1 + \nabla^2)^2)\psi(\vec{x},t) + \psi(\vec{x},t)^3 + V(\vec{x})\right]. \quad (3)$$

Eq. (3) was solved on a 256×256 grid with a spacial discretization $dx = \pi/4$. Analytically, the state of the system can be found by approximating the density with a sum of Fourier modes

$$\psi(\vec{x}) = \sum_{n,m} A_{n,m} \exp\left(i\vec{G}_{m,n} \cdot \vec{x}\right) + \bar{\psi}, \quad (4)$$

where $\vec{G}_{m,n}$ are the relevant reciprocal lattice vectors. The Fourier modes correspond to all possible different symmetries (hexagonal, square, etc.). The density given by Eq. (4) is inserted into the free-energy expression. After integration $F(V_0, \delta_{\rm m}, A_{m,n})$ is then minimized with respect to the coefficients $A_{m,n}$.

3. Results and discussion

3.1. Numerical minimization method

As mentioned above, we find the equilibrium states numerically by solving the equation of motion given by Eq. (3). We start with a hexagonal phase and vary the pinning strength V_0 from 0 to some maximum value, and then we decrease V_0 back to zero. The equilibrium state for each V_0 and $\delta_{\rm m}$ is the one with the lowest energy. Several states were found to minimize the free-energy. For small values of the pinning strength the system is in a hexagonal incommensurate (IC) phase for all mismatches (Fig. 1(a)). If the pinning strength is large enough, the system will be in one of the commensurate phases. The (1×1) phase is an exact match with the pinning potential (Fig. 1(b)).

The other phases are higher commensurate phases which exist only when the relevant reciprocal lattice vectors are close to k_t. One these phases is the c(2×2) phase in which every second site of the lattice of the pinning potential is occupied [5] (Fig. 1(d)). The relevant reciprocal vectors have the

magnitude $k_s/\sqrt{2}$. This state is favored for mismatch values close to $1-\sqrt{2}$ (Fig 2(a)). Another higher commensurate phase is the (2×1) which is generated by a translation of the basis with the reciprocal lattice vectors of the a $\mathrm{c}(2\times 1)$ lattice [5] (Fig. 1(c)). The structure factor ($S(\vec{k}) = \hat{\psi}(\vec{k})\hat{\psi}(-\vec{k})$) of this phase contains a set of peaks corresponding to the (1×1) phase and a set of peaks located between the first and second order peaks of the (1×1) phase. The magnitude of the reciprocal vector which gives the position of this set of peaks is $k_s\sqrt{5}/2$, which suggests that this phase is favored to exist when the mismatch is close to 0.1 (Fig 2(b)). The $(2\sqrt{2}\times\sqrt{2})$ phase is similar to the (2×1) phase. The lattice is generated by a translation of the basis with vectors which are rotated 45° with respect to the pinning potential and the magnitudes of the vectors are $2\sqrt{2}b$ and $\sqrt{2}b$. The structure factor contains a set of peaks corresponding to the $\mathrm{c}(2\times 2)$ phase, while the position of the additional peaks is given by a vectors with magnitude $k_s\sqrt{10}/4$. The phase is favored for mismatch values close to -0.27 (Fig 2(a)).

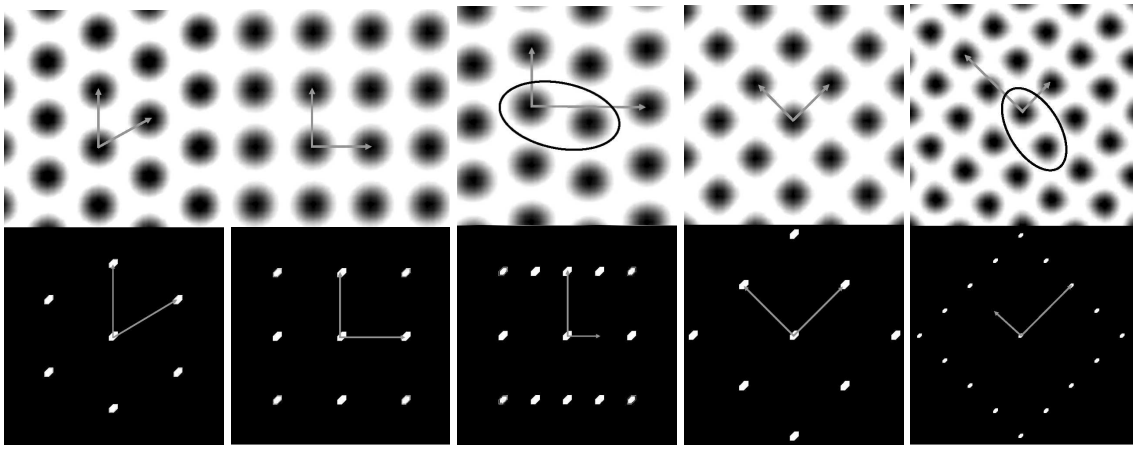

Figure 1. The phases that minimize the free-energy: a) hexagonal, b) square (1×1), c) square (2×1), d) square $\mathrm{c}(2\times 2)$, and e) square $2\sqrt{2}\times\sqrt{2}$. The upper panels represent the density plotted in a gray colormap and the corresponding lattice vectors, while the lower panels the structure factors and the relevant reciprocal lattice vectors. The black contours in Figs. 1(c) and 1(e) show the bases which generate the (2×1) and $(2\sqrt{2}\times\sqrt{2})$ lattices.

The transitions between the different phases are found by investigating the positions and the heights of the peaks in the structure factor. The transitions from IC to any of the commensurate phases and from $\mathrm{c}(2\times 2)$ to (1×1) are discontinuous because these involve a change in the symmetry and/or lattice constant, while the transitions from (2×1) to (1×1) and from $(2\sqrt{2}\times\sqrt{2})$ to $\mathrm{c}(2\times 2)$ appear to be continuous. In this case the magnitude of the additional peaks decrease continuously to zero when the pinning strength is increased. A complete diagram of all these phases is shown in Fig. 2(a) for $\delta_\mathrm{m} < 0$ and in Fig. 2(b) for $\delta_\mathrm{m} > 0$.

3.2. Fourier expansion of the density

In the analytical method we consider the density to be a sum of hexagonal ($A_t(\cos(q_t x)\cos(q_t y/\sqrt(3)) - \frac{1}{2}\cos(2q_t y/\sqrt(3)))$ and square modes, ($A_{s1}\cos(k_s x) + \cos(k_s y)) + A_{s2}\cos(k_s x)\cos(k_s y)$), where $q_t = 2\pi/a_t$. After the integration the free-energy is minimized with respect to the amplitudes A_t, A_{s1}, and A_{s2}. The transition from IC phase to a commensurate phase occurs when $A_t = 0$. In this expansion the transition from IC phase to commensurate phase is discontinuous. This approximation gives good agreement with the numerical minimization for very small and very large values of the pinning strength. The boundary between the IC phase and (1×1) phase is shown in Figs. (2(a) and 2(b)).

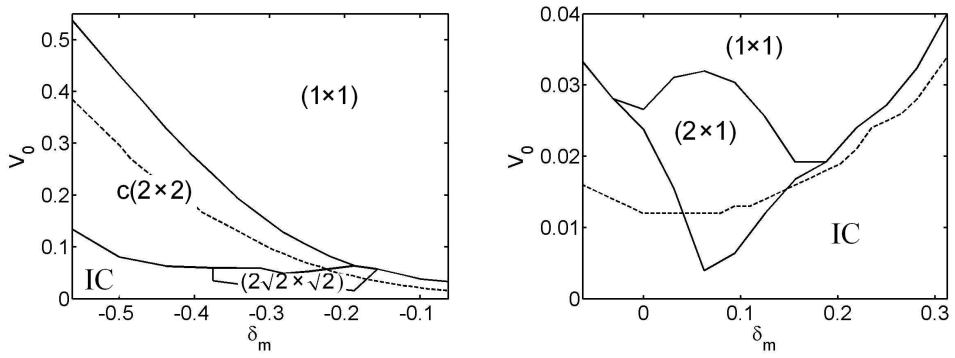

Figure 2. The phase diagram in terms of pinning strength (V_0) and mismatch $\delta_{\rm m}$ for a) $\delta_{\rm m} < 0$ and b) $\delta_{\rm m} > 0$. The dashed lines in a) and b) show the analytical prediction for the boundary between the IC phase and the (1x1) phase. The solid lines show the boundaries between the different phases found by numerical minimization.

4. Conclusions

In this work we extended the research started in Ref. [6]. Detailed phase diagrams of the PFC model in the presence of an external pinning potential are presented for positive and negative mismatch using a numerical minimization of the free-energy. An analytical Fourier expansion of the density provides with us with a qualitative estimate of the transition, but numerical simulations were needed to study the other phases present as well as the phase diagram. The transitions between different phases where found to be discontinuous for IC-(1×1) and c(2×2)-(1×1),while continuous for (2×1)-(1×1) and $(2\sqrt{2} \times \sqrt{2})$-c$(2 \times 2)$. Additional work is required in order to determine the true nature of the different phase transitions by adding thermal fluctuations. Thermal fluctions can be included by adding a noise term in the equations of motion with zero mean and correlation chosen to insure thermal equilibrium at a finite temperature [8] or by Monte Carlo methods [9]. Another particularly interesting application of the model is to pinned driven systems such as in sliding friction of adsorbed layers [10, 11].

5. Acknowledgments

This work supported been supported by a joint fund under EU STREP 016447 MagDot and NSF (DMR-0502737), the Academy of Finland (C.V.A.,T.A.N.), NSF (DMR-0413062) (K.R.E.) and NSERC of Canada (M.K.).

References

[1] Bak P 1982 *Rep. Prog. Phys.* **45** 587
[2] Karttunen M, Haataja M, Elder K R and Grant M 1999 *Phys. Rev. Lett.* **83** 3518
[3] Grüner G 1994 *Density Waves in Solids* (Boston: Addison Wesley Longman)
[4] Koshelev A E and Vinokur V M 1994 *Phys. Rev. Lett.* **73** 3580
[5] Shick M 1981 *Prog. Surf. Sci.* **11** 245
[6] Achim C V, Karttunen M, Elder K R, Granato E, Ala-Nissila T and Ying S C 2006 *Phys. Rev.* E **74** 021104
[7] Elder K R and Grant M. 2004 *Phys. Rev.* E **70** 051605
[8] Elder K R, Katakowski M, Haataja M and Grant M 2002 *Phys. Rev. Lett.* **88** 245701
[9] Ramos J A P, Achim C V, Elder K R, Granato E, Ying S C and Ala-Nissila T *Ordered structures and phase transitions in a phase field crystal model for adsorbed layers*, unpublished.
[10] Persson B N J 1993 *Phys. Rev. Lett.* **71** 1212
[11] Granato E and Ying S C 2000 *Phys. Rev. Lett.* **85** 5368